

# Whitecap coverage in coastal environment for steady and unsteady wave field conditions

C. Lafon, J. Piazzola\*, P. Forget, S. Despiau

*LSEET-LEPI, Université du Sud Toulon-Var, CNRS (UMR 6017) France*

Received 28 October 2005; accepted 12 February 2006

Available online 3 October 2006

## Abstract

Breaking waves represent a “key” parameter for many applications involved with a large number of environmental phenomena. In particular, it is well recognized that the whitecap cover induced by breaking waves allows substantial enhancement of heat, momentum, gas and particle transfer at the air–sea interface. A large number of studies were conducted during the last decades on the variation of the whitecap fraction, commonly noted  $W$ . The results presented in this paper deal with the evolution of the whitecap coverage in coastal zone. In such areas, the wave field is often unsteady with an important variety of sea state developments. The present analysis is based on an extensive series of data obtained during an experimental campaign which took place on the Mediterranean coast in 2001. The results allow observation of the influence of the sea state conditions of the wave field on the whitecap coverage. In addition, this paper confirms the occurrence of a peak in the variations of the whitecap fraction with the wave age for coastal areas as suggested by Lafon et al. [Lafon, C., Piazzola, J., Forget, P., Le Calvé, O. and Despiau, S., 2004. Analysis of the variations of the whitecap fraction as measured in a coastal zone. *Boundary-Layer Meteorol.*, 111: 339–360.]. A wave age dependent model for the whitecap fraction is then proposed, which takes into account both the wind and the wave influence, and hence, is characteristics of the different sea state conditions.

© 2006 Elsevier B.V. All rights reserved.

*Key word index:* Whitecap coverage; Air–sea interactions; Wind–waves; Fetch; Wave age

## 1. Introduction

Under the influence of winds, oceanic currents and solar radiance, the air–sea interface is characterized by a continuous transfer of heat, momentum, gas and particles, which plays an important role in the earth’s climate. It is well recognized that these transfers are substantially enhanced by breaking waves. Indeed, most of the gas exchanges at the sea surface occur in the breaking zones (Liss and Merlivat, 1986; Erikson, 1993;

Asher and Wanninkhof, 1998). The whitecap then plays a major role in the regulating of CO<sub>2</sub> and, hence, on the associated global warming effect through the storage capacity of oceans as the excess of the carbon is shifted back into the atmosphere (e.g., Banner and Peregrine, 1993). In addition, knowledge of wave breaking is of primary importance in many other geophysical applications. For example, it is of great interest for the achievement of a satisfactory sea state model (e.g., Snyder and Kennedy, 1983). The breaking zones also influence both the roughness and the reflectivity of the sea surface and affect the observation by satellite radiometers, as well as the brightness temperature of the sea surface (Weissman

\* Corresponding author.

E-mail address: [piazzola@univ-tln.fr](mailto:piazzola@univ-tln.fr) (J. Piazzola).

et al., 1984; Smith et al., 1992; Wu, 1999). The breaking zone is also involved with the generation of marine aerosol which has a great influence on heat and humidity transfers (Andreas, 1992) and on atmospheric pollution (Fitzgerald, 1991).

Studies concerning the whitecap coverage have started in the sixties with the work of Blanchard (1963). Since, substantial improvement in the knowledge of the variation of the whitecap coverage was obtained following the results published by E. Monahan in which the variation of the sea surface covered by whitecap was described in terms of wind speed and friction velocity (Monahan and O’Muircheartaigh, 1980; Monahan et al., 1983). However, it is now recognized that other factors play a role in the wave breaking, such as the wind–waves interactions, the air–sea temperature difference, the sea surface temperature, the wind action duration, the fetch, the salinity, the surfactants and probably the concentration of dissolved organic materials (e.g.: Toba and Koga, 1986; Monahan and O’Muircheartaigh, 1986; Kraan et al., 1996; Xu et al., 2000; Asher et al., 2002; Stramska and Petelski, 2003). Among these, the fetch represents a major factor through its influence on the development of the wave field. Relatively few studies have been published on the influence of the fetch on whitecap coverage (Snyder and Kennedy, 1983; Xu et al., 2000; Piazzola et al., 2002). Piazzola et al. (2002) showed that most of the models for the whitecap fraction published in the literature agree for long fetches, but disagree dramatically at short fetches.

This paper presents an analysis of the whitecap fraction,  $W$ , in coastal zones as measured during the experimental campaign EMMA (Etat de Mer et Modé-

lisation de l’Aérosol) which took place on a French Mediterranean coast in 2001. One of the objectives of the present study is to address the evolution of the whitecap fraction for developing wave fields. Previous data recorded in the Mediterranean suggested a specific variation of the breaking rate during periods of growing wave (Lafon et al., 2004). Indeed, they note the occurrence of a peak in the variations of the whitecap fraction with wave age for wave age between 5 and 15. However, there were not a sufficient number of data to investigate accurately this range of wave age. The present results confirm the paper by Lafon et al. (2004) and we propose a model for the whitecap fraction for developing wave fields.

## 2. Field site, instrumentation and methods

The experimental data were collected during the EMMA campaign which took place from October 24th to November 22nd 2001 in the Toulon-Hyères bay (Fig. 1) on the French Riviera. The measurement station was located west off the Porquerolles Island. Meteorological sensors were fixed at the top of a 10 m high mast and recorded wind speed and direction, air temperature, relative humidity and pressure. One buoy was moored close to the station (2 km west) and another one 10 km south of the Porquerolles Island. These buoys provided wave measurements from which the wave spectrum were determined.

The whitecap ratio  $W$  (%) was calculated from sea surface photographs taken from the meteorological mast. The camera used was a Canon model EOS 500 and looks at the horizon, slightly downwards. Determination of the

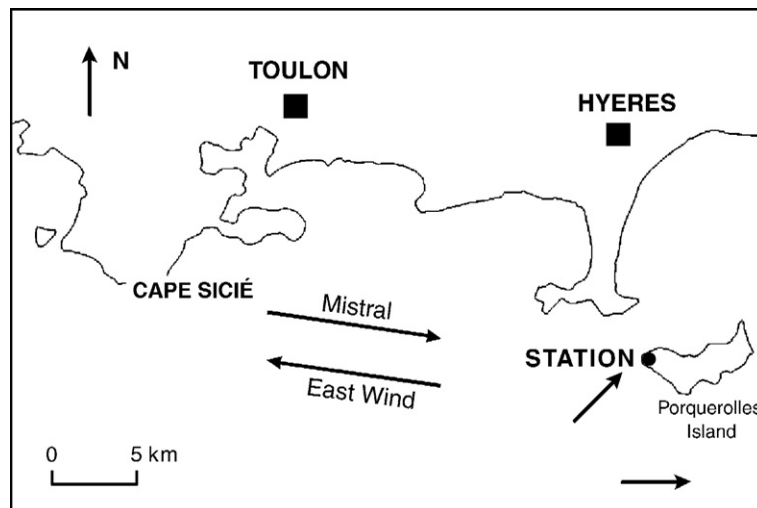


Fig. 1. Detailed view of the studied area. The arrows show the location of the two buoys.

whitecap ratio,  $W$ , was made using an original image processing technique developed at the laboratory (Mas-souh and Le Calve, 1999). The method consists of a robust and automatic processing technique based on the image digitization and grey scale conversion. The whitecap value is obtained using a numerical method for detecting the closed contours of the whitecap areas from the photographs (Fig. 2). The intensity threshold to separate whitecaps from the rest of the sea surface is evaluated from the image gradient. A simplification of the geometrical transformation was developed to make corrections for the perspective effect and to convert the image pixels into surface units. Effect of the sun is manually corrected.

A single whitecap fraction value generally corresponds to 24 pictures taken every 30 s. Error is reduced by analyzing only the middle of each photograph. In addition, precision of the whitecap data was statistically considered by reducing the uncertainties of the regression models (see Section 4) using the standard deviation of the series of the photographs in accordance with the methodology proposed by Monahan (1971). A standard deviation value is calculated on each mean whitecap value. The accuracy of the mean whitecap value for a given sequence has been estimated by dividing the standard deviation by a factor equal to the square root of one less than the number of photographs used to determine that data point.

The values obtained by this method represent the total whitecap area, i.e., whitecaps of stage A and B, as defined by Monahan and Woolf (1989) since the treatment includes foam.

Analysis of both the meteorological and the sea state conditions is important to evaluate the state of development of the wave field. Fetch-limited conditions correspond to a steady wave field, where wave parameters depend on both the wind speed and the fetch length.

Duration-limited conditions correspond to stationary meteorological conditions and unstationary wave field conditions. To ensure the conditions of equilibrium of the sea state, we used the criterion which defines duration-limited conditions of the wave field (e.g., Hsu, 1986) reported in Section 4 (see Eq. (7)). In the latter case, wave parameters depend on both the wind speed and the fetch but also on the wind duration. According to Young (1999) duration-limited conditions correspond to the development of the wave field over a calm sea for a spatially homogeneous wind constant in intensity and direction. These conditions are rarely met in an oceanic environment (Young, 1999). In the coastal zone, the wind direction represents an important parameter which directly influences both the production and the dispersion of the particles through the influence of fetch (Piazzola and Despiau, 1997). In the present study, winds blowing from Northwest to Northeast correspond to short fetches (less than 30 km), while the Southwest to Southeast directions correspond to longer fetches. By considering the data recorded during episodes of wind speeds larger than 5 m/s only, the dominant winds were blowing from the Northwest–West directions. These winds correspond to the northwest winds, namely called Mistral. Mistral is a cold and dry wind that gustily blows during several days and which is associated with unclouded weather. Mistral is often associated with Tramontane, which designates winds blowing from West (Mayençon, 1992).

### 3. Previous models for the whitecap fraction

One of the objectives of the present study is to provide an expression for the whitecap fraction for partially developed wave fields. The occurrence of whitecapping is directly related to the mechanical transfer of momentum



Fig. 2. The numerical method for detecting the closed contours of the whitecap areas from the photograph.

from the wind to the sea surface through the wind stress  $\tau = -\rho u'w'$  (where  $u'$  and  $w'$  are the horizontal and the vertical fluctuations of the wind speed, respectively) that generates waves. Although the first models were only wind speed dependent (e.g., Monahan and O'Muircheartaigh, 1980), a parameterisation of  $W$  versus the friction velocity  $u_*$  which includes turbulence effects and the atmospheric stability (Monahan and O'Muircheartaigh, 1986; Monahan and Woolf, 1989) was also proposed. The wind speed dependent model generally used is (Monahan and O'Muircheartaigh, 1980):

$$W(\%) = 2.95 \cdot 10^{-4} U_{10}^{3.52} \quad (1)$$

Under the assumption of equilibrium of the wave field, Wu (1988) proposed:

$$W(\%) = 20 \cdot u_*^3 \quad (2)$$

On the basis of tank data and dimensional arguments, Toba and Koga (1986) proposed an alternative expression for the whitecap fraction which also involves an explicit dependence to the sea state through the wave peak frequency  $f_p$ . This model has been recently modified by Zhao and Toba (2001) who proposed:

$$W(\%) = 3.88 \cdot 10^{-5} (R_B)^{1.09} \quad (3)$$

where  $R_B = u_*^2 / 2\pi\nu f_p$  is a dimensionless parameter obtained by combining the dimensionless friction velocity  $u_*^* = u_*^3 / g\nu$  (where  $g$  is the gravity acceleration and  $\nu$  is the kinematic viscosity of sea water) and the dimensionless peak frequency ( $f_p^* = u_* f_p / g$ ).

The wave age represents a convenient parameter to characterize wave growth under a constant wind speed. It is then used in a large number of parameterisations of the wind drag coefficient,  $C_D$ , the roughness length,  $z_0$ , and the momentum flux over wind waves (e.g., Geernaert et al., 1987; Maat et al., 1991; Toba and Ebuchi, 1991; Lin et al., 2002; Drennan et al., 2003). The general definition of the wave age is the ratio between the phase velocity of the dominant wave,  $c_p$ , and the wind speed:  $\zeta = c_p / U_{10} \cos \theta$ , where  $\theta$  is the angle between the wind and the wave direction. Generally, one considers that  $\theta \approx 0$ . The wave age can also be written in terms of wind stress, i.e.,  $\zeta_* = c_p / u_*$ . Young waves occur as the wind starts to blow over a calm sea. They are characterized by a high peak frequency, and in turn, a rather small phase velocity. As the wind is blowing, the wave age increases until an equilibrium is reached which corresponds to fetch-limited or fully-developed sea state conditions for large fetches. For young waves, i.e.,  $\zeta < 1$

and  $5 < \zeta_* < 15$  (e.g., Janssen, 1994; Young, 1999), the energy balance is dominated by the momentum transfer from the wind to the wave field. This corresponds to a period of enhancement of the wave energy. In contrast, for mature waves, i.e.,  $\zeta \approx 1$  and  $25 \leq \zeta_* \leq 30$ , the energy input from the wind to the waves is balanced by dissipation process through wave breaking and the wave energy remains constant. Large wave ages correspond to weakening wind waves and/or the occurrence of long swell, whereas small wave ages correspond to active wind waves in a growing phase (Geernaert et al., 1987). Toba et al. (1990) suggest a realistic interval of wave ages for wind waves:  $0.003 \leq c_p / U_{10} \leq 1.0$ . Kraan et al. (1996) showed that the active part of the whitecap coverage can be modelled by:

$$W = 96(\zeta_*)^{-2.08} \quad (4)$$

On the basis of the data collected during the FETCH experiment (Hauser et al., 2003), Lafon et al. (2004) showed that for larger wave ages i.e.,  $\zeta_* \geq 15$ , the variation of the whitecap fraction is in accordance with the predictions of Eq. (4).

On the basis of the model of Snyder and Kennedy (1983), Xu et al. (2000) proposed a fetch dependent model for  $W$  an expression that relates the whitecap coverage to the dimensionless fetch length  $\tilde{X}$ :

$$W(\%) = 1 - \Phi(0.29\tilde{X}^{0.25}) \quad (5)$$

$$\Phi(z) = \frac{1}{\sqrt{2\pi}} \int_{-\infty}^z \exp(-y^2/2) dy.$$

where  $\tilde{X}$  is the nondimensional fetch, i.e.,  $gX / U_{10}^2$  with  $X$  the geometrical fetch.

#### 4. Results

The EMMA campaign allowed for an extensive series of photographs resulting in 29 significant values of whitecap percentage (Table 1). The wave parameters were continuously recorded near the meteorological station where photographs of the sea surface were collected. The values of the friction velocity,  $u_*$ , reported in Table 1 were obtained using a linear wind speed dependent expression of the wind drag coefficient specifically established in a coastal North Mediterranean area during FETCH experiment as (Dupuis et al., 2003):

$$C_{DN} = 0.56 + 0.063 U_{10} \quad \text{for } 6 < U_{10} < 19 \text{ ms}^{-1} \quad (6)$$

where  $C_{DN}$  is the wind drag coefficient in neutral air stratification conditions.

Table 1

Values of the whitecap percentage encountered during the EMMA campaign and the measured parameters, i.e., wind speed, friction velocity; wave peak frequency and significant wave height

Day/time	$U_{10}$ (m/s)	$u_*$ (m/s)	$f_p$ (Hz)	$H_S$ (m)	$W$ (%)
24/10 12 h22	10.5	0.35	0.168	1.4	0.93
24/10 13 h02	11.2	0.39	0.210	1.5	1.73
24/10 14 h00	12.2	0.44	0.180	1.6	1.88
24/10 15 h00	12.5	0.47	0.161	1.8	1.45
24/10 16 h00	11.6	0.41	0.152	1.9	0.81
04/11 14 h13	10.0	0.33	0.298	0.7	0.84
04/11 15 h12	10.1	0.33	0.261	0.7	0.41
05/11 14 h10	10.9	0.37	0.249	1.0	0.34
05/11 15 h11	11.1	0.39	0.260	0.9	0.37
06/11 10 h51	14.8	0.57	0.198	1.3	0.055
07/11 08 h33	15.7	0.65	0.141	2.1	2.08
07/11 09 h36	15.0	0.61	0.139	2.3	2.54
07/11 10 h40	16.1	0.68	0.130	2.5	2.11
07/11 11 h39	16.2	0.69	0.138	2.4	4.68
07/11 12 h45	17.9	0.80	0.132	2.3	4.09
07/11 13 h42	14.2	0.56	0.150	2.4	3.24
07/11 14 h41	14.1	0.56	0.138	2.5	1.97
08/11 08 h45	12.1	0.44	0.157	1.9	0.47
08/11 09 h45	11.4	0.40	0.140	1.9	0.43
08/11 10 h45	13.2	0.51	0.141	2.3	1.23
08/11 11 h46	14.7	0.59	0.138	2.4	3.84
08/11 12 h45	14.9	0.61	0.140	2.4	2.99
08/11 13 h45	15.7	0.66	0.148	2.2	3.32
08/11 14 h45	16.1	0.68	0.142	2.3	4.01
09/11 08 h41	11.2	0.39	0.140	1.6	0.4
09/11 09 h41	14.1	0.56	0.142	1.9	1.76
09/11 10 h41	14.1	0.56	0.149	1.9	2.16
09/11 11 h41	14.1	0.56	0.141	1.8	2.7
09/11 12 h41	11.2	0.39	0.160	1.7	1.73

Measurements of the whitecap fraction  $W$  were performed during Mistral episodes. In Figs. 3–7 the variation of the whitecap fraction versus the different available parameters i.e.,  $U_{10}$ ,  $u_*$ ,  $R_B$ ,  $c_p/U_{10}$  and  $c_p/u_*$  are reported. First, our analysis will focus on data measured during steady events. Next section will deal with the whole dataset. The steadiness of the wave field was estimated using the following criterion for duration-limited growth as expressed by Hsu, 1986:

$$gt/U_{10} = 68.8\tilde{X}^{0.667} \quad (7)$$

where  $t$  is the minimum duration for the waves to be in equilibrium with the wind.

4.1. Whitecap coverage for steady wave field conditions

Most of the models for the whitecap fraction  $W$  published in the literature, as those reported in Eqs. (1)–(5), refer to equilibrium conditions of the wave field. Figs. 3–7 allow for comparison of the whitecap fraction measured

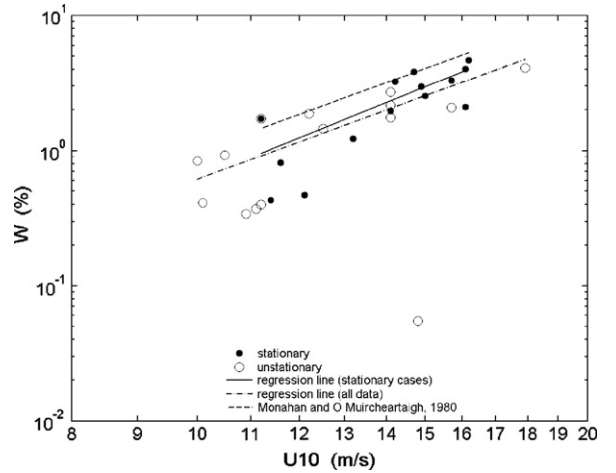


Fig. 3. Variation of the whitecap data measured during the EMMA experiments versus wind speed measured at 10 m height,  $U_{10}$ . The black circles show the data points recorded during steady conditions of the wave field, while the white ones deal with unsteady conditions of the wave field. The full line shows the regression calculated only for the steady data, while the dash-dot line represents the regression plot on the whole data set. The dashed line plots the model by Monahan and O’Muircheartaigh (1980).

during steady events of the EMMA campaign to these models, except for the fetch dependent model reported in Eq. (5) that we have not plotted. The discrepancies observed between the EMMA data and such a fetch dependent model are explained by the difficulty of knowing the exact value of the effective fetch for certain wind

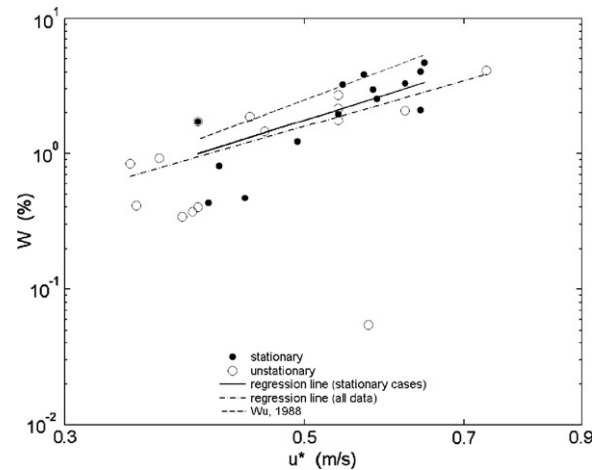


Fig. 4. Variation of the whitecap data measured during the EMMA experiments versus wind friction velocity,  $u_*$ . The black circles show the data points recorded during steady conditions of the wave field, while the white ones deal with unsteady conditions of the wave field. The full line shows the regression calculated only for the steady data, while the dash-dot line represents the regression plot on the whole data set. The dashed line plots the model by Wu (1988).

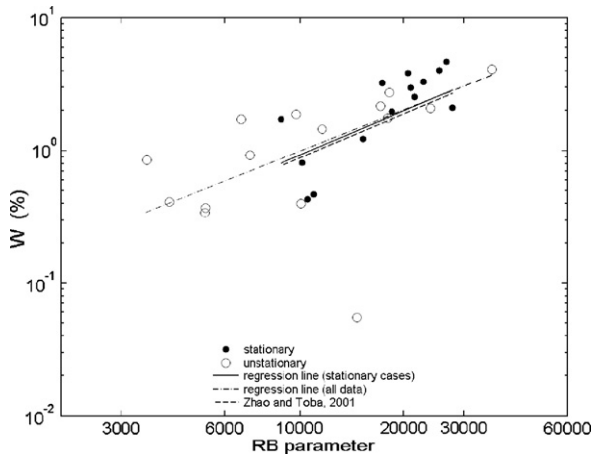


Fig. 5. Variation of the whitecap data measured during the EMMA experiments versus  $R_B = u_*^2 / 2\pi v_f^2$  (see in the text). The black circles show the data points recorded during steady conditions of the wave field, while the white ones deal with unsteady conditions of the wave field. The full line shows the regression calculated only for the steady data, while the dash-dot line represents the regression plot on the whole data set. The dashed line plots the model by Zhao and Toba (2001).

conditions, due to the complexity of the coastline in the region. This difficulty to estimate the real fetch did not allow us to test our data against a fetch dependent parameterisation as this proposed by Xu et al. (2000). Using Figs. 3–6, the empirical relationships between  $W$  and some of the different parameters are given by:

$$W(\%) = 8.1 \times 10^{-5} U_{10}^{3.88} \quad (8)$$

$$W(\%) = 10.2 \times u_*^{2.53} \quad (9)$$

$$W(\%) = 3.7 \times 10^{-5} (R_B)^{1.10} \quad (10)$$

$$W(\%) = 0.54 \times (\zeta)^{-5.75} \quad (11)$$

The corresponding correlation coefficients are  $r=0.823$ ,  $r=0.823$ ,  $r=0.8$ ,  $r=0.844$ , respectively.

For a wave field in equilibrium, our whitecap data are well correlated to any of wind/wave parameter considered. It is clear that the whitecap coverage depends on the wind speed, but the coefficients obtained for the  $W-U_{10}$  relationships in the present paper are different from those obtained by Monahan and O’Muircheartaigh (1980) and those obtained in previous results in the Mediterranean published by Lafon et al. (2004). Seasonal variation of the sea surface temperature may also play a role on the whitecap coverage through its influence on bubble distributions (e.g., Walsh and Mulhearn, 1987), the rate of the viscous dissipation processes (Donelan and Pierson, 1987) and the exponential decay time of a single whitecap (e.g., Monahan, 1985; Ponder, 1986). For comparison, the model reported in Eq. (1) was

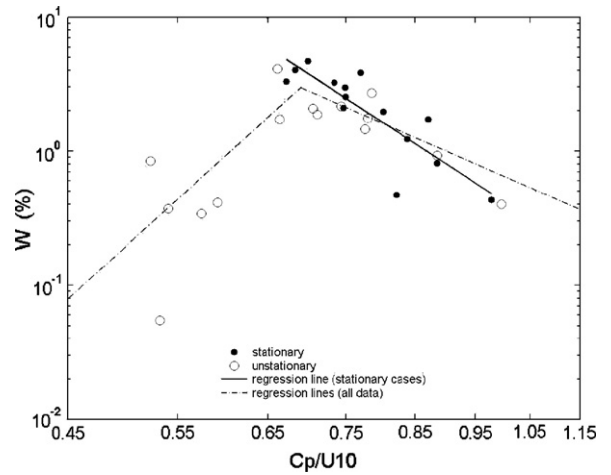


Fig. 6. Variation of the whitecap data measured during the EMMA experiments versus wave age,  $\zeta = c_p / U_{10}$ . The black circles show the data points recorded during steady conditions of the wave field, while the white ones deal with unsteady conditions of the wave field.

established on the basis of data recorded in warm waters with a temperature larger than 25 °C, while the present data correspond to a sea surface temperature around 14 °C. This can also explain the differences in the whitecap coverage measured with our data and Eq. (1). Differences are also observed for the coefficients in the  $W-u_*$  relationship (Eq. (9)) while Eq. (10) shows a good agreement for the  $W-R_B$  relationship between our data and the model proposed by Zhao and Toba (2001). In addition, Fig. 6 shows that the whitecap ratio  $W$  decreases with the wave age as suggested by Kraan et al. (1996).

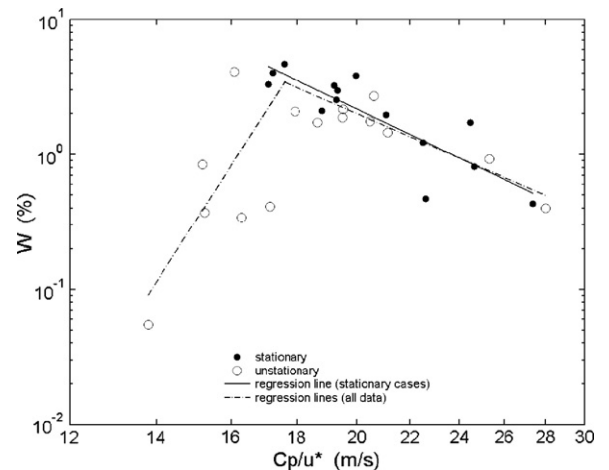


Fig. 7. Variation of the whitecap data measured during the EMMA experiments versus wave age,  $\zeta_* = c_p / u_*$ . The black circles show the data points recorded during steady conditions of the wave field, while the white ones deal with unsteady conditions of the wave field.

#### 4.2. Influence of sea state conditions

Analysis of the complete data set, including unsteady state conditions of the wave field, allowed observation of the influence of the sea state development on the evolution of the whitecap ratio (see Figs. 3–7). For both the wind speed and the friction velocity, the empirical relationships corresponding to the data fit leads to:

$$W(\%) = 1.90 \times 10^{-4} U_{10}^{3.51} \quad (12)$$

$$W(\%) = 7.78 \times u_*^{2.29} \quad (13)$$

The correlation coefficients for Eqs. (12) and (13) are  $r=0.571$  for both.

In accordance with observations in Figs. 3 and 4, the coefficients of the data fit are different compared to those reported in the previous section. This confirms that the wind speed dependency differs for the unsteady events. Fig. 6 shows the variation of the whitecap fraction  $W$  with the wave age  $c_p/U_{10}$ . We note a peak for a wave age around 0.7. Below 0.7, the whitecap coverage tends to increase with  $\zeta = c_p/U_{10}$ , while it decreases for higher wave ages. The empirical relationships calculated on the data fit in Fig. 5 are expressed by:

$$W(\%) = \begin{cases} 70 \times \zeta^{8.5} & \text{for } \zeta \leq 0.69 \\ 0.65 \times \zeta^{-4.1} & \text{for } \zeta > 0.69 \end{cases} \quad (14)$$

The correlation coefficients are  $r=0.878$  and  $r=0.8$ , respectively.

Fig. 7 shows the variation of  $W$  versus the wave age calculated using the friction velocity. We note a peak which occurs for a  $\zeta_*$  between 16 and 18. However, this value can vary slightly since it depends on the wind drag coefficient used to determine the friction velocity. A similar peak using direct measurements of  $u_*$ , was observed around 15 in the FETCH data (Lafon et al., 2004). As noted, calculations of the wind friction velocity  $u_*$  were obtained using the wind drag coefficient reported in Eq. (6), which was established on the basis of the Mediterranean FETCH experiment by Hauser et al. (2003). For comparison, calculations were made using four different expressions for the wind drag coefficient and show that the peak is always located between 16 and 19 (Lafon, 2004).

Figs. 6 and 7 then confirm the results obtained in the previous study made on the Mediterranean area by Lafon et al. (2004) which suggested a peak in the variation of the whitecap fraction versus the wave age. In addition, the two distinct portions which occur in Figs. 6 and 7 are consistent with the results reported in the literature for the variation of both the wind stress and the whitecap ratio with respect to the development of the wave field.

The peak in the wind stress–wave age plot reported in recent studies (e.g.: Nordeng, 1991; Donelan et al., 1993; Makin and Kudryavtsev, 2002) occurs generally in the range between 5 and 15. In addition, the variation with wave age of the growth wave parameter, which is defined as the ratio between the energy flux and the energy of the waves (e.g., Townsend, 1972) shows a peak at a wave age around 15. This is in accordance with the data of Kraan et al. (1996), who also observed whitecap values for wave age smaller than 15.

#### 4.3. Model of the whitecap fraction $W$ for coastal areas

The data recorded during the EMMA campaign showed that the influence of the wind on the whitecap fraction varies with respect to the equilibrium state of the wave field. In particular, the highly unsteady event is not accurately represented by most of the parameterisations of  $W$ . In addition, the values of the coefficients exhibited in the relationships used for comparison differ from those obtained in a nearby Mediterranean coastal zone during the FETCH campaign (Lafon et al., 2004). These differences of the coefficient values are in accordance with the variety of the results published in the literature and is probably related to the variety of the local conditions of the data set considered for the different studies. This shows that the wind speed dependence in the whitecap modeling is probably not sufficient to account for all the wind–wave coupling processes involved with the whitecapping. For example, the Monahan and O’Muircheartaigh (1980) model globally overestimates the present data. This can be explained by the fact that  $W$  is quite difficult to model for unsteady conditions by classical variables such as wind speed. Indeed, for unsteady conditions, the whitecap coverage can then be small even for high wind speeds, while it can be large for low wind speeds during a period of wave decay. This is one of the reasons why Stramska and Petelski (2003), by using data recorded in polar North Atlantic, proposed different relationships between the whitecap fraction  $W$  and the wind speed  $U_{10}$  according to the state of development of the wave field, i.e., for developed seas and undeveloped seas.

By using the inertio-dissipative method to estimate the friction velocity, Lafon et al. (2004) showed that the  $W-u_*^3$  relationship predicts well the variation of the whitecap fraction even when the wave field equilibrium is not reached. However, Stramska and Petelski (2003) showed that the scatter of the whitecap coverage data was not improved when  $u_*$  is used instead of  $U_{10}$ . When the friction velocity  $u_*$  cannot be measured, as for the present study, it is difficult to know which expression to take for the wind drag coefficient  $C_D$ . In this case, the

parameterisation function of  $U$  will be preferred. In particular, for parameterisation using the wave age,  $\zeta$  would be rather used than  $\zeta_*$ . Indeed, to model the whitecap ratio for highly unsteady conditions of the wave field, the wave age represents a relevant parameter. The Mediterranean data show that the  $W$ – $\zeta$  relationship takes into account all the situations encountered, and is independent of the  $u_*$  uncertainties. In the case of a complex sea state, the coupling between ocean and atmosphere is well taken into account with  $\zeta$  (see discussion).

## 5. Discussion and conclusion

This paper presents an analysis of the whitecap fraction,  $W$ , measured in a Mediterranean coastal zone. We note a least correlation between the whitecap data recorded during unsteady state conditions of the wave field and both the wind speed and the friction velocity (Eqs. (8) and (9) compared to the whole dataset which includes data recorded for unsteady conditions of the wave field (Eqs. (12) and (13)). Unsteady conditions correspond to periods of amplification (or attenuation) of the wave energy before an equilibrium is reached between the wave field and the wind input, as already noted previously (Lafon et al., 2004). In this case, the whitecap coverage can be small even at high wind speeds before the equilibrium between waves and wind is reached, while the whitecap coverage can be large for low wind speeds during a period of wave attenuation (Lafon et al., 2004). In addition, these kinds of conditions often correspond to the case of a wind blowing over a complex wave field. This induces a lower reliability for the fetch dependent model for the whitecap fraction since in many cases the effective fetch generating the wave field does not correspond to the distance to the coastline in the wind direction. For example, Sugihara et al. (2005) note that the presence of swell contaminates the fetch-dependence of whitecap. The present results (Eqs. (12) and (13)) show that the wind speed and the friction velocity dependent models lose accuracy for unsteady conditions of the wave field. A quite good description of such developing wave fields can be provided by a study of the air–sea interaction processes using the wave age parameter, which characterizes well the development of the wave field.

The results presented in this paper confirm the occurrence of a peak in the variation of the whitecap fraction with the wave age as suggested by Lafon et al. (2004). This shows a similar behaviour of the variation of the whitecap ratio with respect to the wave age for both the wind stress (e.g., Nordeng) and the wave growth rate (Townsend, 1972; Belcher and Hunt, 1998). The present results allow determination of a new wave age dependent

model for the whitecap coverage (Eq. 14). The variations of  $W$  in the decreasing phase appear more clearly as in the increasing one, for which the dispersion of the data is much larger. That can be explained by the fact that some of the wave fields corresponding to very small wave age (especially for wave ages lower than the peak value) are characteristic of highly unsteady conditions. In that case, situations of cross seas that correspond to young waves (since wave age is calculated using the wind sea peak frequency) can exist. The whitecap cover could then be due to the breaking of wind waves, but also to interactions with the residual swell.

## Acknowledgements

The authors wish to thank Dr. R. Van Hooff for the corrections of the early draft of the manuscript and the staff at the EMMA campaign, in particular Tathy Missamou. This work was supported by the French Ministry of Research.

## References

- Andreas, E.L., 1992. Sea spray and the turbulent air–sea heat fluxes. *J. Geophys. Res.* 97 (C7), 11429–11441.
- Asher, W.E., Wanninkhof, R., 1998. The effect of bubble-mediated gas transfer on purposeful dual gaseous-tracer experiments. *J. Geophys. Res.* 103, 10,555–10,560.
- Asher, W.E., Edson, J.B., McGillis, W.R., Wanninkhof, R., Ho, D.T., Litchendorf, T., 2002. Fractional area whitecap coverage and air–sea gas transfer during GasEx-98. In: Donelan, M.A., Drennan, W.M., Saltzman, E.S., Wanninkhof, R. (Eds.), *Gas Transfer at Water Surfaces*. American Geophysical Union, Washington D.C., pp. 199–204.
- Banner, M.L., Peregrine, D.H., 1993. Wave breaking in deep water. *Annu. Rev. Fluid Mech.* 25, 373–395.
- Belcher, S.E., Hunt, J.C.R., 1998. Turbulent flow over hills and waves. *Ann. Rev. Fluid Mech.* 30, 507–538.
- Blanchard, D.C., 1963. The electrification of the atmosphere by particles from bubbles in the sea. *Progress in Oceanography*, vol. 1. Pergamon Press, New York, pp. 71–202.
- Donelan, M.A., Pierson Jr., W.J., 1987. Radar scattering and equilibrium ranges in wind-generated waves—with application to scatterometry. *J. Geophys. Res.—Oceans* 92 (C5), 4971–5029.
- Donelan, M.A., Dobson, F.W., Smith, S.D., Anderson, R.J., 1993. On the dependence of sea surface roughness on wave development. *J. Phys. Oceanogr.* 23, 2143–2149.
- Drennan, W.M., Graber, H.C., Hauser, D., Quentin, C., 2003. On the wave age dependence of wind stress over pure wind seas. *J. Geophys. Res.* 108 (C3) (FET10-1 to FET 10-13).
- Dupuis, H., Guerin, C., Hauser, D., Weill, A., Nacass, P., Drennan, W.M., Cloché, S., Graber, H.C., 2003. Impact of flow distortion corrections on turbulent fluxes estimated by the inertial dissipation method during the FETCH experiment on R/V Atalante. *J. Geophys. Res.* 108 (C3) (FET 12-1 to FET 12-17).
- Erikson III, D.J., 1993. A stability dependent theory for air–sea gas exchange. *J. Geophys. Res.* 98, 8471–8488.

- Fitzgerald, J.W., 1991. Marine aerosols: a review. *Atmos. Environ.* 25 A, 523–545.
- Geernaert, G.L., Larsen, S.E., Hansen, F., 1987. Measurements of the wind stress, heat flux, and turbulence intensity during storm conditions over the North Sea. *J. Geophys. Res.* 92 (C12), 13 127–13 139.
- Hauser, D., Branger, H., Bouffies-Cloch e, S., Despiau, S., Drennan, W.M., Dupuis, H., Durand, P., Durrieu de Madron, X., Estournel, C., Eymard, L., Flamant, C., Graber, H.C., Gu erin, C., Kahma, K., Lachaud, G., Lef evre, J.-M., Petterson, H., Pignat, B., Queff eulou, P., Tailliez, D., Tournadre, J., Weill, A., 2003. The FETCH experiment: an overview. *J. Geophys. Res.* 108 (C3), 8053, doi:10.1029/2001JC001202.
- Hsu, S.A., 1986. A mechanism for the increase of wind stress (drag) coefficient with wind speed over water surfaces: a parametric model. *J. Phys. Oceanogr.* 16, 144–150.
- Janssen, P.A.E.M., 1994. Wave growth by wind. In: Komen, et al. (Eds.), *Dynamics and Modelling of Ocean Waves*. Cambridge University Press, pp. 71–112.
- Kraan, C., Oost, W.A., Janssen, P.A.E.M., 1996. Wave energy dissipation by whitecaps. *J. Atmos. Ocean. Technol.* 13, 262–267.
- Lafon, C., 2004. Evaluation du taux de d ef erlement en zone c ot iere M editerran enne. PhD Thesis, Southern University of Toulon-Var, France, pp. 205.
- Lafon, C., Piazzola, J., Forget, P., Le Calv e, O., Despiau, S., 2004. Analysis of the variations of the whitecap fraction as measured in a coastal zone. *Boundary - Layer Meteorol.* 111, 339–360.
- Lin, W., Sanford, L.P., Suttles, S.E., 2002. Drag coefficient with fetch-limited wind waves. *J. Phys. Oceanogr.* 32, 3058–3074.
- Liss, P.S., Merlivat, L., 1986. Air–sea exchange rates: introduction and synthesis. In: Buat-Menard, P. (Ed.), *The Role of Air–Sea Exchange in Geochemical Cycling*. D. Reidel, pp. 113–127.
- Maat, N., Kraan, C., Oost, W.A., 1991. The roughness of wind waves. *Boundary - Layer Meteorol.* 54, 89–103.
- Makin, V.K., Kudryavtsev, V.N., 2002. Impact of dominant waves on sea drag. *Boundary - Layer Meteorol.* 103, 83–99.
- Massouh, L., Le Calve, O., 1999. Measurement of whitecap coverage during F.E.T.C.H. 98 experiment. 1999 European Aerosol Conference, Prague, Czech Republic, September 6–10 1999. *J. Aerosol Sci.* 30 (suppl.1), s177–s178.
- Mayen on, R., 1992. *M eteorologie Marine*. Ed. Maritimes et d’Outre-Mer, Edilarge S.A.
- Monahan, E.C., 1971. Oceanic whitecaps. *J. Phys. Oceanogr.* 1, 139–144.
- Monahan, E.C., 1985. The Ocean as a Source for Atmospheric Particles. NATO Advanced Study Institute Conference on the Role of Air–Sea Exchange. *Geochemical Cycling*. Reidel, Dordrecht.
- Monahan, E.C., O’Muircheartaigh, I.G., 1980. Optimal power-law description of oceanic whitecap coverage dependence on wind speed. *J. Phys. Oceanogr.* 10, 2094–2099.
- Monahan, E.C., O’Muircheartaigh, I.G., 1986. Review article: whitecaps and the passive remote sensing of the ocean surface. *Int. J. Remote Sens.* 7 (5), 627–642.
- Monahan, E.C., Woolf, D.K., 1989. Comments on “Variations of Whitecap Coverage with Wind Stress and Water Temperature”. *J. Phys. Oceanogr.* 19, 706–709.
- Monahan, E.C., Fairall, C.W., Davidson, K.L., Boyle, P.J., 1983. Observed interrelation between 10 m winds, ocean whitecaps and marine aerosols. *Q. J. R. Meteorol. Soc.* 109, 375–392.
- Nordeng, T.E., 1991. On the wave age dependent drag coefficient and roughness length at sea. *J. Geophys. Res.* 96 (C4), 7167–7174.
- Piazzola, J., Despiau, S., 1997. Contribution of marine aerosols in the particle size distributions observed in Mediterranean coastal zone. *Atmos. Environ.* 31, 2991–3009.
- Piazzola, J., Forget, P., Despiau, S., 2002. A sea spray generation function for fetch-limited conditions. *Ann. Geophys.* 20 (11), 121–131.
- Pounder, C., 1986. Sodium chloride and water temperature effects on bubbles. In: Monahan, E.C., MacNiocail, G. (Eds.), *Oceanic Whitecaps and their Role in Air–Sea Exchange Processes*. Reidel Publishing Company, p. 278.
- Smith, S.D., Anderson, R.J., Oost, W.A., Kraan, C., Maat, N., De Cosmo, J., Katsaros, K.B., Davidson, K.L., Bumke, K., Hasse, L., Chadwick, H.M., 1992. Sea surface wind stress and drag coefficients: the HEXOS results. *Boundary - Layer Meteorol.* 60, 109–142.
- Snyder, R.L., Kennedy, R.M., 1983. On the formation of whitecaps by a threshold mechanism, part I, Basic formalism. *J. Phys. Oceanogr.* 13, 1482–1492.
- Stramska, M., Petelski, T., 2003. Observations of oceanic whitecaps in the north polar waters of the Atlantic. *J. Geophys. Res.* 108 (C3), 3086, doi:10.1029/2002JC001321 (pp. 31-1 to 31-10).
- Sugihara, Y., Tsumori, H., Ohga, T., Yoshioka, H., Serizawa, S., 2005. Variation of whitecap coverage with wave-field conditions, Li ege Colloquium on ocean dynamics. *Gas Transfer at Water Surfaces*. May 2–6.
- Toba, Y., Ebuchi, N., 1991. Sea-surface roughness length fluctuating in concert with wind and waves. *J. Oceanogr. Soc. Jpn.* 47, 63–79.
- Toba, Y., Koga, M., 1986. A parameter describing overall conditions of wave breaking, whitecapping, sea-spray production and wind stress. In: Monahan, E.C., Mac Niocail, G. (Eds.), *Oceanic Whitecaps and Their Role in Air–Sea Exchange Processes*. Reidel Publishing Company, pp. 37–47.
- Toba, Y., Iida, N., Kawamura, H., Ebuchi, N., Jones, I.S.F., 1990. Wave dependence of sea-surface wind stress. *J. Phys. Oceanogr.* 20, 705–721.
- Townsend, A.A., 1972. Flow in a deep turbulent boundary layer over a surface distorted by water waves. *J. Fluid Mech.* 55, 719–735.
- Walsh, A.L., Mulhearn, P.J., 1987. Photographic measurements of bubble populations from breaking wind waves at sea. *J. Geophys. Res.* 92, 14,553–14,565.
- Weissman, M.A., Atakt urk, S.S., Katsaros, K.B., 1984. Detection of breaking events in a wind-generated wave field. *J. Phys. Oceanogr.* 14, 1608–1619.
- Wu, J., 1988. Notes and correspondence: “Variations of Whitecap Coverage with Wind Stress and Water Temperature”. *J. Phys. Oceanogr.* 18, 1448–1453.
- Wu, J., 1999. On wave dependency of altimeter sea returns — weak fetch influence on short ocean waves. *J. Atmos. Ocean. Technol.* 16, 373–378.
- Xu, D., Liu, X., Yu, D., 2000. Probability of wave breaking and whitecap coverage in a fetch-limited sea. *J. Geophys. Res.* 105 (C6), 14,253–14,259.
- Young, I.R., 1999. *Wind Generated Ocean Waves*. Elsevier Ocean Engineering Book Series, p. 306.
- Zhao, D., Toba, Y., 2001. Dependence of whitecap coverage on wave and wind–wave properties. *J. Oceanogr.* 57, 603–616.